Egyptian Journal of Petroleum (2016) 25, 323–332

Egyptian Petroleum Research Institute

Egyptian Journal of Petroleum

www.elsevier.com/locate/egyjp
www.sciencedirect.com

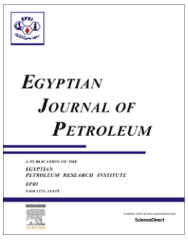

FULL LENGTH ARTICLE

Electrical, mineralogical, geochemical and provenance of Cretaceous black shales, Red Sea Coast, Egypt

Esmat A. Abou El-Anwar [a], **Mohamed M. Gomaa** [b,*]

[a] *National Research Center, Geological Sciences Dept., Cairo, Egypt*
[b] *National Research Center, Geophysical Sciences Dept., Cairo, Egypt*

Received 22 April 2015; revised 27 July 2015; accepted 3 August 2015
Available online 18 December 2015

KEYWORDS

Dielectric constant;
Conductivity;
Frequency domain;
Black shales;
Geochemistry;
Pollution

Abstract Detailed mineralogical and geochemical studies were carried out on the middle members of the black shales of the Duwi Formation (Quseir–Safaga province) to define their source rock, paleo-weathering, pollution impact and provenance of the sources. The studied black shales are highly fossiliferous and fissile. They are texturally classified as phosphatic marly mudstone microfacies. The black shale mineral composition is mainly composed of calcite, apatite, quartz, pyrite and clay minerals. The average values of Cu, Ni, Zn, Cr, V, As and Se and the ratios Rb/Sr and Cr/Ni in black shale are enriched compared to those of the Post-Archean Australian Shale (PAAS) values. Electrical properties of samples were measured using a non-polarizing electrode, at room temperature (~18 °C), and relative atmospheric humidity of (~35%), in the frequency range from 42 Hz to 5 MHz. The changes in electrical properties were argued to be due to the change in mineral composition. Generally, the electrical properties of rocks are changed due to many factors such as grain size, mineral composition, grain shape and inter-granular relations between grains. The dielectric constant decreases with frequency, and increases with conductor concentration. Also, the conductivity increases with the increase of conductor continuous paths between electrodes.

1. Introduction

Electrical properties can be useful for the interpretation of frequency spectra of the complex dielectric constant or conductivity of rocks and porous materials in general, and for the determination of the connectivity of channels and their lengths. Egyptian carbonaceous shales have drawn attention because of their geological and economic significance (as a source rock and raw material). The black shales in Egypt gained interest since five decades when the phosphorite deposits were discovered and exploited. The interest in black shales all over the world in the last decades principally stems from the

* Corresponding author. Fax: +20 00233370931.
E-mail address: mmmsgomaa@yahoo.com (M.M. Gomaa).
Peer review under responsibility of Egyptian Petroleum Research Institute.

http://dx.doi.org/10.1016/j.ejpe.2015.08.006

widespread recognition that black shales are important source rocks of petroleum or may be used as natural fuel resources.

Phosphorites are intercalated with and capped by black shales. They contain considerable amounts of organic matter and are enriched in trace elements, which may be of economic potential. Upper Cretaceous sediments in the southern Egypt consist of variegated shales upon which, a thick sedimentary succession follows. The sediments are of shallow marine origin with some lateral and vertical lithological changes, in which the phosphate deposits are, intercalated [1]. The black shales are hosted mainly in the Campanian to Maastrichtian Duwi and Dakhla formations. The compositions of shales could provide information on the tectonic setting, provenance, weathering conditions, and sediment recycling. The present study concerns with electrical, mineralogical and geochemical characters of the black shales in the Quseir–Safaga area, Red Sea coast in order to discus their pollution pattern, provenance and the paleo-weathering depositional environment. The chosen area is located at longitudes 34° 03′ 12″–34° 03′ 24″ E and latitudes 26° 11′ 27″–26° 11′ 37″ N (Fig. 1).

The monitoring of electrical properties can be very useful for the control of pollution, oil reservoir monitoring, hydrothermal energy and exploration of the deep earth and exploration of the shallow earthquake prediction studies and so on. Correct interpretation of field data calls for a clear understanding of possible sources of variations of electrical properties. This is a very delicate problem as electrical properties of porous media such as conductivity, dielectric constant and electrochemical potentials are extremely sensitive to physical conditions, the chemical composition of solid and liquid phases, and microstructural factors (porosity, its distribution and its connectivity).

Generally, increase of conductive paths between the electrodes increases the conductivity and the dielectric constant [2,3]. Electrical properties (conductivity, dielectric constant and impedance) depend on the charge density on grains, grain shape, grain size, the conductor concentration, the properties of electrolyte (conductivity and dielectric constant), and the measured frequency value [4,5]. With an increase of insulator concentration or insulator continuous paths the dielectric constant value decreases. There is a critical percolation threshold with the increase of conductor concentration. At that percolation threshold the continuous paths begin to contact with each other, forming conducting paths between electrodes and accordingly more conductivity values are added [6,7].

The present work aims to provide detailed, electrical, mineralogical, geochemical, and petrographical information and to determine the economic potential of some Egyptian Carbonaceous shales. Also, this study is a tool showing more details on the relation between the geochemical composition of the measured samples through electrical laboratory measurements (conductivity and dielectric constant as a function of frequency).

2. Geology

The Formation in the Quseir–Safaga region is of Campanian age in its lower part and Maastrichtian in the upper part [1]. Baioumy and Ismael [8] classify the Duwi Formation in the Red Sea area into four members. The middle member ranges in thickness from 5 to 12 m. It is characterized by soft, yellowish-gray laminated shales. They are intercalated with 2–25 cm-thick, yellowish-gray, massive, hard, coarse-grained siliceous phosphorites. The studied middle member of this formation is composed of dark gray, highly fossiliferous and fissile shales. The breakdown of organic matter and pyrite increase the fissility. The dark color revealed to presence of more than 1% organic matter (maceral).

3. Materials and methodology

To achieve this study, 7 samples from the middle member of the Duwi Formation were selected to represent the black shales in the studied area. Representative samples were collected from the shale beds. Mineralogically, selected samples were investigated by the X-ray technique, at the Metallurgical Center for Research and Development Institute, Tebbin, Egypt, using a Phillips X-ray diffraction model, with Ni-filtered Cu-K α radiation. For the clay mineral investigations, after removal of carbonate and organic matter 0 mg of the suspended (<2 μm) fraction was used to prepare three oriented particle mounts (untreated, glycolated and heated). SEM investigation for the surface texture of the clayey size grains of the selected samples are carried out in the Egyptian mineral resources authority (Central Laboratories). The major and

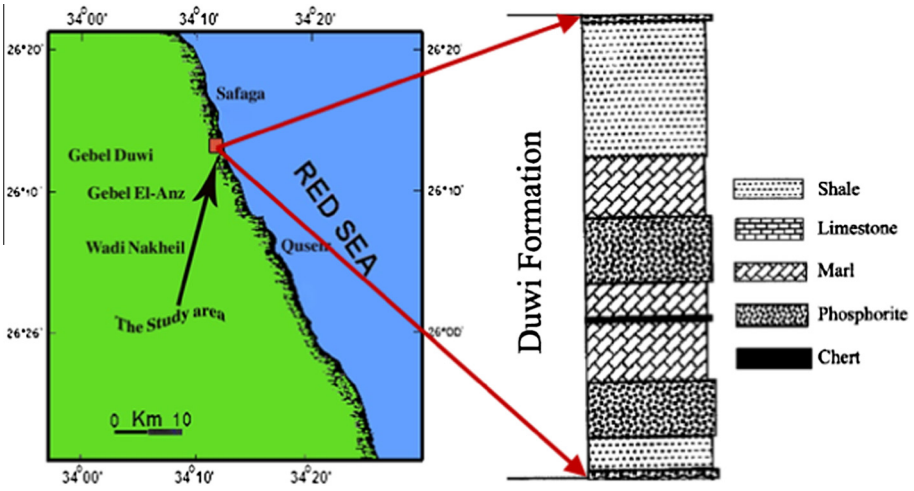

Figure 1 Shows location map of the studied area in addition to the lithostratigraphic section of the area.

trace elements of some selected samples were analyzed by XRF to determine the chemical composition by using Axios Sequential WD_XRD Spectrometer, Analytical 2005 in the National Research Center laboratories, Egypt.

Hioki 3522-50 LCR Hitester impedance analyzer was used to measure the electrical properties (dielectric constant, conductivity, impedance). The geometry of samples for electrical measurements was chosen to reduce errors due to stray capacitance. The sample edges were polished to be parallel. Samples cover all the studied area. Electrical properties were measured in the frequency range from 42 Hz to 5 MHz, using non-polarizing electrodes ($Cu/CuSO_4$) at oscillation amplitude of 1 volt [9].

Electrical properties of samples may be measured in either the series or parallel configuration. Parameters were measured using parallel capacitance and conductance (C_p and G_p) and series impedance Z at different frequencies. Complex relative dielectric constant is $\varepsilon^* = \varepsilon' - i\varepsilon''$, where, $\varepsilon' = C_p d/\varepsilon_0 A$, is the real part of complex relative dielectric constant before correction and the imaginary part of complex relative dielectric constant is $\varepsilon'' = G_p d/\omega\varepsilon_0 A$, where A is the cross-sectional area of the sample, d is the sample thickness, $\varepsilon_0 = 8.85 \times 10^{-12}$ is the free space permittivity and ω is the angular frequency. The real conductivity is $\sigma' = G_p d/A = \varepsilon''\omega\varepsilon_0$.

Electrical properties were measured in an isolated chamber at relative atmospheric humidity of (~35%) at room temperature (~18 °C) (desiccator) [10,11]. Correction due to fringing for capacitance can be used through the formula of Chew and Kong 1980. The electrode impedance was found to be in the order of (15-J 0.1) Ω within used frequency range and it was removed from measurements [4].

4. Results and discussion

4.1. Petrography

The studied samples were described as phosphatic marly mudstone microfacies. They are characterized by their black color, and highly phosphatic fossil content. The bioclastics are represented by planktonic foraminifera (such as: globigerina, gastroboda), algae and organic matter (maceral) scattered in micritic matrix (Fig. 2A). The abundance of planktonic foraminifera gives evidence of middle to inner shelf marine environment. Apatite is the main constituent of the phosphatic component in the studied samples. It is represented by biophases (bone fragments, spines and teeth of vertebrates such as fish) and collophane which is isotropic and occurs as grains, peloids and coprolites (Fig. 2B–D). Framboidal pyrite is disseminated in irregular masses and clusters of different shapes and sizes (Fig. 2A). The dominant occurrence of the framboids, particularly the clustered forms, in shales tends to indicate a biogenic origin as a consequence of the bacterial reduction of seawater sulphate. Framboidal pyrites are the result of the weathering and diagenetic processes [12]. Black shales are deposited predominantly in oxygen minimum zones, where depositional environments are characterized by low current speed and low oxygen level, favoring the preservation of organic matter.

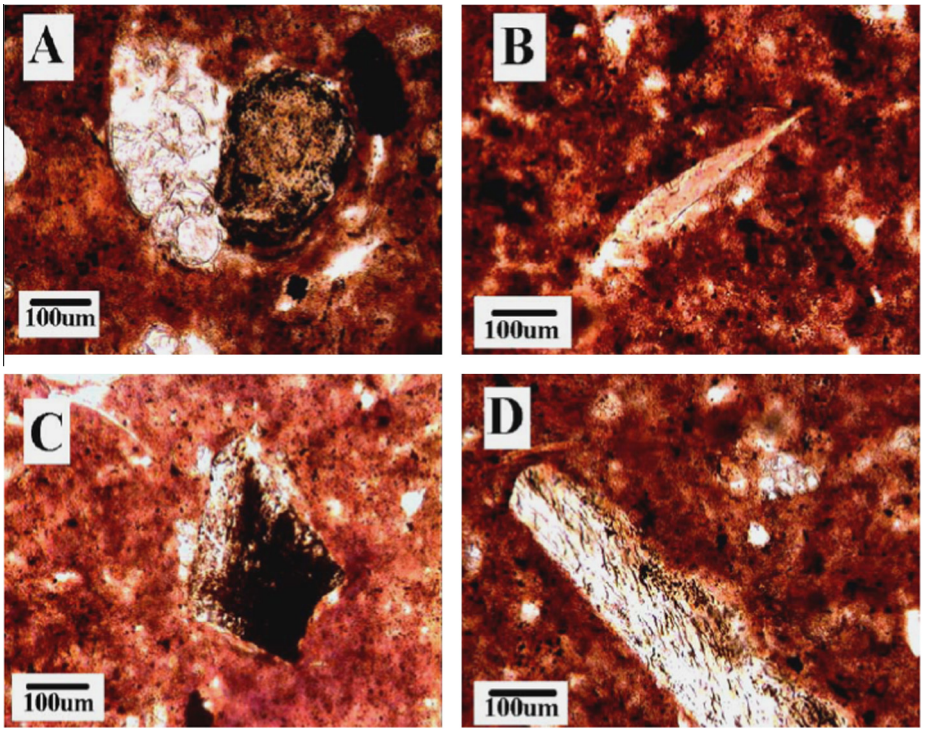

Figure 2 (A) The petrography of completely pyritized foraminiferal (globigerina) tests and clusters of pseudomorphosed framboidal pyrite embedded in organic-rich mudstone, S. No. 2., P.P.L. (B) shows apatitic spine together with maceral embedded in micritic matrix, S. No. 4, P.P.L. (C) shows apatitic bone fragments embedded in organic-rich mudstone, S. No. 5, P.P.L. (D) showing syngenetic apatitic skeletal fragment concentrating pyrite inside skeletal bones, S. No. 7, P.P.L.

4.2. Mineralogy

4.2.1. Clay minerals

X-ray analysis revealed that the dominant clay minerals in the studied clay fraction are mainly montmorillonite, mixed layer montmorillonite-illite and minor kaolinite (Fig. 3). The predominant montmorillonite is Na- montmorillonite as indicated from XRD which can be compared to the bentonite composition. SEM examination is confirmed with the dominance of montmorillonite (Fig. 4A–C) and the mixed layer of montmorillonite-illite (Fig. 4D). The montmorillonite occurs as detrital and is of authigenic origin (Fig. 4A–D).

4.2.2. Non-clay minerals

The X-ray analysis revealed that samples are composed mainly of calcite, fluorapatite (francolite), quartz and pyrite. From petrographic studies, the presence of calcite and foraminifers' fossils revealed that the deposition was in a marine environment. Pyrite, occurs as framboids, is extensively pseudomorphosed into goethite and/or hematite that is formed as authigenic deposits. The presence of pyrite as spheres may be a marker indicator of shallow water on submarine in shelf settings (Fig. 4C and D).

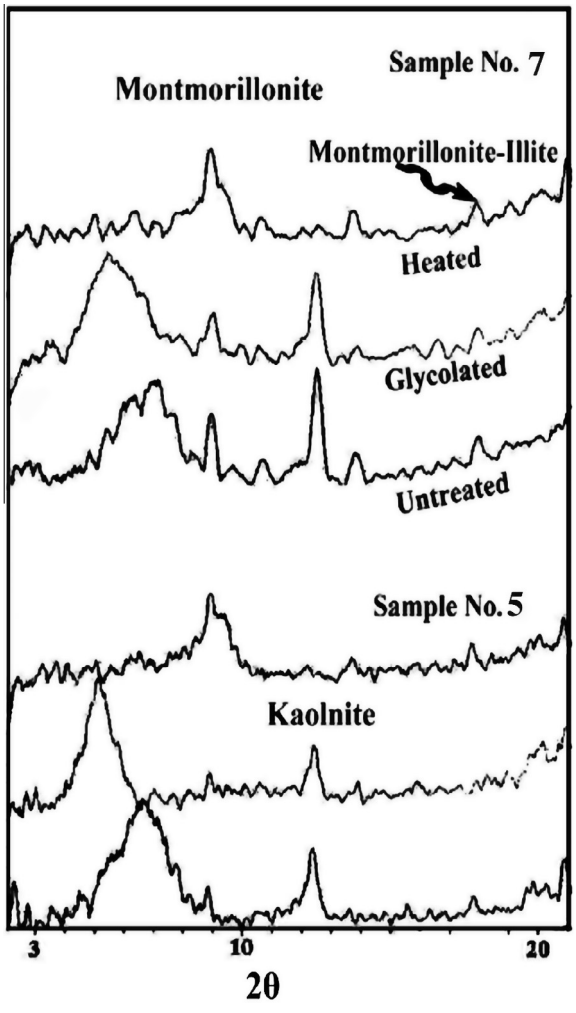

Figure 3 Shows X-ray diffraction pattern of the studied black shales. It shows the presence of montmorillonite-illite, montmorillonite and Kaolinite in the samples.

4.3. Geochemistry

Geochemical composition (major and trace elements), along with their ratios for five selected samples are shown in (Table 1).

4.3.1. Major elements

CaO is the dominant constituent of the studied black shale samples (~21.4%, Table 1). This average value is relatively comparable to the average marine black shales of the red sea area [8]. SiO_2 and Al_2O_3 are the second abundant elements (~15.89%). The SiO_2/Al_2O_3 ratios are (~3.01%) and are nearly close to that of pure montmorillonite (~2.8–3.31%); this is confirmed with the XRD and SEM results. The K_2O/Al_2O_3 ratios are (~0.08–0.09%). The mean value of P_2O_5 is ~3.42%. MgO concentrations are ~0.64%. The sulfur concentration is ~7.24%. Recognition of sulfur in the form of framboidal pyrite suggests microbial activity under euxinic conditions. Titanium concentration is ~0.33%. Concentrations of K_2O and Na_2O are (~0.45% and ~0.13%, respectively) (see Fig. 5).

4.3.2. Trace and rare earth elements

Vanadium is the most abundant trace element in the studied samples (~2331 ppm). The high concentration of *V* may be due to oxidation and weathering of the organic matter. *Zinc* is the second abundant trace element in samples (~1230 ppm). The studied shales contain high concentrations of *Ni* (~375 ppm). The high values of *Ni* show that it is deposited under marine condition (up to 300 ppm; [13]). The average *Pb* content is ~11 ppm. *Zr* content is ~886 ppm (Fig. 6). *Strontium* content is ~677 ppm. The high Sr content may be due to the presence of aragonitic fossils and shells, as well as by the primary apatite in bones and teeth of vertebrates [14–16]. *Selenium* concentration is ~43 ppm. Terrigenous input and volcanic activity are possible sources for Se and the other metals such as V, Ni, Mo, Cu, Mo and Zn in black shales. Consequently, the secondary hydrothermal or supergene solutions are good markers for the enrichment in the studied black shales. *Yttrium* concentration is ~30 ppm. The commonly immobile elements; Al, Fe, Ti, Th, Sc, Co, Cr, and their ratios, are useful markers of provenance such as weathering, transportation and sorting [17]. Generally, the trace elements; Cr, V, Zn, Zr, Ni, Cu, Se and As are enriched more in other localities (Fig. 6).

4.3.3. Organic richness

The black shales for the studied middle member of the Duwi Formation have organic matter (OM) ~17.8%, (Table 1). This value is relatively comparable to those values of the marine black shales of the Red Sea area (~16.6%, [8]). However, it is obviously higher than the compared values for the average of the Duwi Formation and Dakhla Formation (0.95% and 1.33%; respectively) [18], and the TOC content (4.35%) of the transgressive Dakhla Formation. Consequently, the studied black shales can be classified as good to excellent source of oil [19], which is similar to the Lower Silurian shales in China [20]. The microorganisms in black shales revealed the

effect of the organic matter during the chemical weathering [21]. TOC/S ratios significantly above 2.8 suggest sulfur limitation and reduced salinity [22]. Sulfur contents (7.24%) and TOC/S ratios (2.46) are indicated as oxygen restricted conditions similar to the marine Carboniferous shales in Britain [23].

4.4. Provenance and paleoenvironment

4.4.1. Source rocks

The concentration of the transitional metals is used for the differentiation of the nature and composition of source rocks. The mafic rocks have higher Cr, Ni, Cu, Zn and V concentrations compared to those of felsic rocks. Consequently, the higher contents of Cr, Ni, Cu, Zn and V as well as Sr (739, 375, 215, 1230, 2331 and 677 ppm; respectively) in the studied samples can be attributed to the abundance of mafic volcanic rocks in the source rocks and intensive chemical weathering, [24,25]. Mafic components from the basement source rocks may be accumulated during weathering and probably derived from the basement terrains in the Red Sea Hills.

The high enrichments of trace elements in sedimentary rocks such as V, Cr, Ni, As, Sr, Mo, and Cd, are believed to be related to the hydrothermal activity [26,27]. The enrichment of these trace elements in the studied black shales indicated that the depositional process may have been coupled with submarine hydrothermal activity derived from ancient, mafic rocks. On the other hand, the contents of zirconium (~886 ppm) in the studied black shales and TiO_2/Zr ratios (~2.42–21) reveal that a felsic source rock is the most probably additional source rock. In fact, it is suggested that the studied area was subjected to intensive weathering which led to intensive strong pollution. Due to the incorporation between pollution and organic matter, weather causes the high concentration of it. The enrichment of Zr may, also, be attributed to the granite and the Nubian sandstones transported from the red sea hills.

4.4.2. Climatic conditions and sediment maturity

The original characters and maturity of the sediments together with the prevailed climatic conditions can be recognized by calculating ICV (Index Compositional Variation) proposed by [28]:

$$ICV = (Fe_2O_3 + K_2O + Na_2O + CaO + MgO + MnO)/Al_2O_3.$$

The ICV tends to be highest in minerals high in the weathering intensity and decreases in more stable minerals. The ICV decreases further in the montmorillonite group clay minerals and is lowest in the kaolinite group minerals [28]. Also, the more mature shales exhibit low ICV values (< 1.0). For the studied shales, the calculated ICV value ranges from 0.82 to 1.0 (Table 1). Consequently, these shales are considered to be highly mature. The K_2O/Na_2O ratios are 3.48. These ratios revealed the high maturity of the studied black shales [29, Table 1]. This is confirmed with the ICV values. The K_2O/Na_2O ratios are comparable to those of sediments from passive margins, which increase with maturity of rocks.

4.4.3. Chemical mobility and weathering trends

The chemical composition of the weathering products in a sedimentary basin is expected to reveal the mobility of various elements during weathering. The chemical Index of Alteration (CIA) and the Chemical Index of Weathering (CIW) provide information about the intensity of chemical weathering [30] and are calculated as:

$$CIA = [Al_2O_3/(Al_2O_3 + CaO^* + Na_2O + K_2O)] \times 100$$

$$CIW = [Al_2O_3/(Al_2O_3 + CaO^* + Na_2O)] \times 100$$

The CIA values are ~88. The CIW values are ~95 (Table 1). This average revealed the high intensive chemical weathering

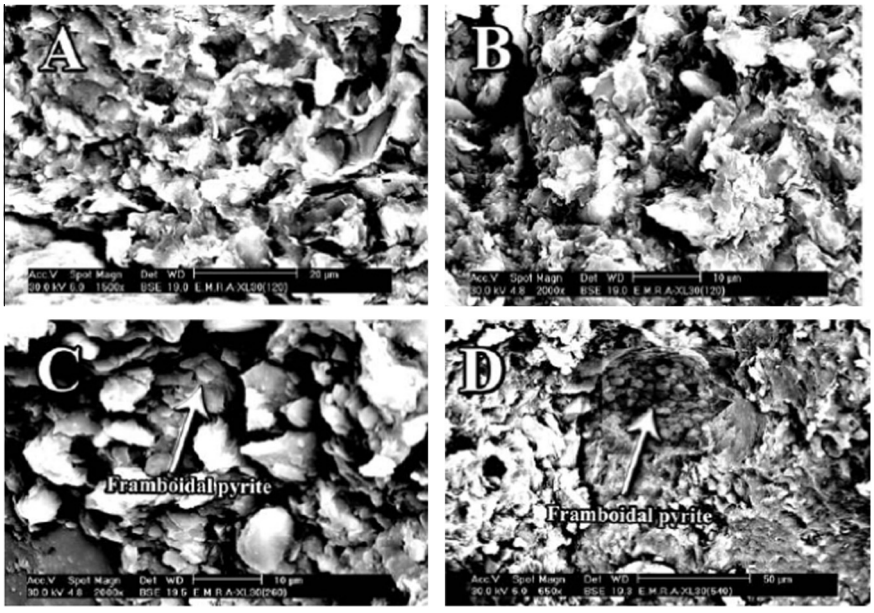

Figure 4 (A) Wavy sheet montmorillonite with sharp edge texture. (B) Sharp edged and crenulated morphology of montmorillonite, (C) Well crystallized montmorillonite with well-developed morphology and framboidal pyrite (authigenic), (D) Mixed layer montmorillonite-illite and framboidal pyrite (authigenic).

[30]. There is a strong weathering indication, which implies the humid paleoclimate [31]. The studied black shales have an average ICV (0.92), and CIA 88.16%. This indicated that the studied shales are geochemically highly mature, and were derived from intensive weathered source rocks. The studied shale samples have an average Rb/Sr ratio of 0.047 (Table 1). This suggests that the degree of the chemical weathering of the source rocks was relatively comparable to the PAAS values [31].

4.4.4. Depositional environments

The studied shale samples are markedly enriched in redox sensitive trace elements; vanadium, zinc, chromium, strontium, molybdenum, nickel, cadmium, selenium and arsenic averaging (2331, 1230, 739, 677, 647, 375, 228, 43 and 19 ppm; respectively). This enrichment is usually related to the anoxic condition [32,33]. The V/Cr ratio has been used as a paleo-oxygenation indicator. The V/Cr ratios for samples are ~3.22 (Table 1), which reveal that it was deposited under anoxic conditions. The V/(V + Ni) ratios are ~0.86 which reveal that it were deposited under relatively euxinic conditions [34]. Consequently, the studied black shales were deposited under relatively euxinic to anoxic marine conditions and coupled with hydrothermal solutions [34,35].

4.4.5. Environmental impact (Geoaccumulation index)

The black shales usually have a high content of organic carbon and sulphides and are important hosts for a remarkable collection of ore metals such as Co, Ni, V, U, Mo, Mn, P, and the platinum group elements [36]. Because of their high organic carbon and sulphide contents, black shales are susceptible to

Table 1 Chemical analysis of major oxides (%) and trace elements (ppm) of black shales. OM = organic matter, ICV = index of compositional variation, CIA = chemical index of alteration, CIW = chemical index of weathering.

Elements	1	2	3	4	5	Maxm.	Minm.	Average
SiO_2	15.44	16.42	16.63	15.83	15.13	16.63	15.13	15.89
TiO_2	0.32	0.34	0.33	0.32	0.34	0.34	0.32	0.33
Al_2O_3	4.92	5.59	5.52	5.28	5.15	5.59	4.92	5.29
Fe_2O_3	3.43	3.67	3.32	3.71	3.91	3.91	3.32	3.61
MnO	0.02	0.02	0.02	0.03	0.02	0.03	0.02	0.02
CuO	0.02	0.03	0.03	0.03	0.02	0.03	0.02	0.03
NiO	0.05	0.05	0.04	0.05	0.05	0.05	0.04	0.05
ZnO	0.15	0.15	0.14	0.14	0.15	0.15	0.14	0.15
Cr_2O_3	0.09	0.12	0.1	0.11	0.12	0.12	0.09	0.11
V_2O_5	0.54	0.28	0.33	0.41	0.52	0.54	0.28	0.44
MgO	0.64	0.65	0.63	0.64	0.65	0.65	0.63	0.64
CaO	21.33	21.68	21.56	21.32	21.1	21.68	21.1	21.4
SrO	0.07	0.08	0.06	0.08	0.09	0.09	0.06	0.08
Na_2O	0.12	0.14	0.13	0.14	0.12	0.14	0.12	0.13
K_2O	0.45	0.45	0.44	0.46	0.45	0.46	0.44	0.45
CdO	0.02	0.03	0.03	0.03	0.02	0.03	0.02	0.03
ZrO_2	0.02	0.2	0.1	0.08	0.2	0.2	0.02	0.12
MoO_3	0.1	0.1	0.1	0.09	0.1	0.1	0.09	0.1
P_2O_5	3.23	3.53	3.22	3.6	3.55	3.6	3.22	3.42
SO_3	7.08	7.33	7.35	7.55	8.1	8.1	7.08	7.24
Cl	0.03	0.03	0.03	0.03	0.03	0.03	0.03	0.03
F	0.25	0.23	0.24	0.26	0.25	0.26	0.23	0.25
LOI	41.68	38.88	39.65	39.81	39.93	41.68	38.88	39.99
OM	17.5	18.4	18.2	17.7	17.2	18.4	17.2	17.8
As	0	23	0	20	40	0	40	17
Pb	0	20	15	10	8	0	20	11
Rb	33	21	25	28	40	21	40	29
Se	42	46	50	45	35	35	50	44
Y	25	33	30	28	35	25	35	30
SiO_2/Al_2O_3	3.14	2.94	3.01	3.00	2.94	3.14	2.94	3.01
MgO/Al_2O_3	0.13	0.12	0.11	0.12	0.13	0.13	0.11	0.12
K_2O/Al_2O_3	0.09	0.08	0.08	0.09	0.09	0.09	0.08	0.09
Al_2O_3/TiO_2	15.38	16.44	16.73	16.50	15.15	16.73	15.15	16.04
K_2O/Na_2O	3.75	3.21	3.38	3.29	3.75	3.75	3.21	3.48
V/(V + Ni)	0.89	0.82	0.85	0.86	0.88	0.89	0.82	0.86
V/Cr	4.9	1.9	2.7	3.05	3.55	4.9	1.9	3.22
Ti/Al	0.07	0.06	0.06	0.06	0.07	0.06	0.06	0.06
TiO_2/Zr	21	2.42	4.46	5.41	2.62	21	2.42	7.18
Rb/Sr	0.056	0.031	0.049	0.041	0.053	0.056	0.031	0.047
Cr/Ni	1.57	2.11	2.17	1.94	2.1	2.17	1.57	1.99
Moppm/Al%	718.9	630.5	633.7	602.3	686.4	718.9	602.3	654.4
ICV	0.95	0.88	0.82	0.94	1.00	1.00	0.82	0.92
CIA	87.70	88.45	88.75	78.71	88.18	88.75	78.71	88.16
CIW	95.35	95.23	95.5	94.96	95.55	94.96	95.55	95.32

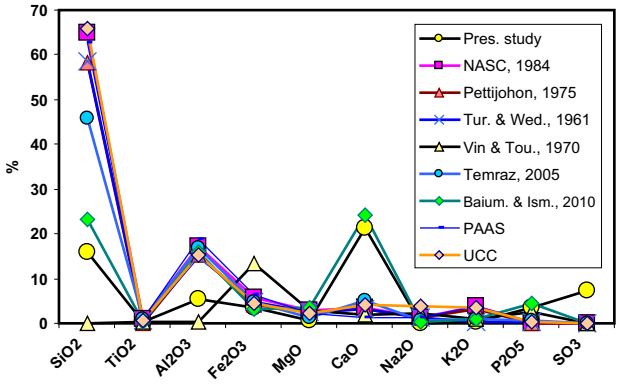

Figure 5 Shows a comparison between compositions of major elements in this study and other published papers of black shales. Pres. Study = present study, NASC = North American Shale Composite, PAAS = Average Post-Archean Australian Shale and UCC = Upper Continental Crust [17].

alteration when exposed. The weathering of black shale is important because of dispersion of toxic metals and the production of acid mine drainage that may affect the ecosystem due to oxidation of sulphides. Such chemical changes are generally explained by mineral dissolution, secondary mineral formation, cation exchange and loss and gain of amorphous oxide phases. Many metals (including Cd, Co, Mn, Mo, Ni, U, Zn, and PGE (platinum group elements) are lost from shales and others are enriched in soils derived from the shales [36,37]. The index of geoaccumulation (Igeo) designed by Müller [38] has been useful to evaluate the contamination of sediments in the environment [39].

$$\text{Igeo} = \log_2(\text{Cn}/1 : 5\text{Bn})$$

where Cn is the measured concentration of the metal in the sample and Bn represents its geochemical background concentration. In this study, the concentrations of elements in the PAAS [17] were used as background values. The geoaccumulation index in relation to the pollution extent is classified into seven classes (Table 2). Applying the geoaccumulation index for the studied samples shows that Si, Ti, Al, Fe, Mn, MgO, Sr, Na, Pb and K, are classified as unpolluted to moderately polluted. Cu, Ni, Rb and Cr are considered as moderately polluted. In addition, P is represented as moderately to strongly polluted where Zn and Ca are classified as strongly polluted. Finally, V, Zr, Cd and Mo recognized as very strong polluted (Fig. 7). These are most probably attributed to the intensive chemical weathering of the source rocks. Generally, the geoaccumulation indexes show that the black shales are unpolluted to very strong polluted.

4.5. Electric

Fig. 8 shows the change of conductivity with frequency. The conductivity increases with the increase of frequency and with the increase of total conductor concentration that leads to the increase of continuous conduction paths in samples. Fig. 9 shows the change of dielectric constant with frequency. The dielectric constant decreases with the increase of frequency and increases with the increase of total conductor concentration in the sample up to a certain limit (percolation threshold) [40]. Above the percolation threshold the dielectric constant decreases with the increase of total conductor concentration in samples. This is due to the blocking of the conductor continuous paths in the samples, which may be related to the high percentage of the organic matter in the samples (up to 18.4). Fig. 10 shows the variation of complex impedance of samples. Measured data of complex impedance show nearly an arc for low conductor samples and with the increase of conductor conduction paths this arc is contracted to be a part of a semicircle. Conductor conduction paths are the summation of different conductor concentrations in the sample. The real and imaginary impedance of the samples decreases with the increase of conductor conduction paths between electrodes (different conductor concentrations).

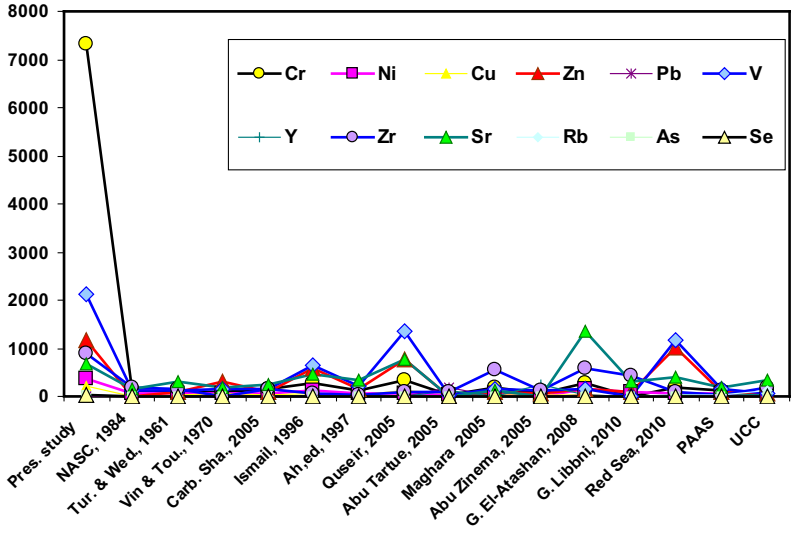

Figure 6 Shows a comparison between compositions of trace elements in this study and other published papers of black shales. Pres. Study = present study, NASC = North American Shale Composite.

Conductivity shows a general trend of increase with frequency, while the general trend of dielectric constant shows a decrease with frequency. It is noticed that the behavior of samples is similar to each other. This may be due to the comparable conductor concentration in the samples and may be due to the homogeneity of the minerals in the samples. Most of the conducting materials in these samples are dispersed and coated with the insulating material that is the reason that most of the samples behave as insulators.

The abrupt variation in conductivity shown in sample 5, may be due to the presence of a direct current continuous path (DC) [41], or due to montmorillonite and the mixed layer of montmorillonite-illite minerals from the X-ray diffraction, Fig. 2]. One slope can be noticed with frequency for all the curves. The conductivity is low at low total conductor concentration and at low frequency. At higher frequencies and higher total conductor concentration, more continuous conductor paths exist between grains that lead to the relative increase of conductivity values [42,43]. The increase of frequency motivates particles to overcome barriers between energy levels to form continuous conductor paths between the grains and accordingly the conductivity increases [44].

Relatively high values of dielectric constant in the samples may be due to the presence of conducting grains coated by insulator materials [such as the organic matter] or may be attributed to the small pores between grains in the samples (small grain size clay minerals). Also, the dielectric constant increases from one sample to another due to the increase of the fluctuations of concentrations of the insulating materials between the conducting grains. With the increase of the conducting material, the insulating gaps decrease and the dielectric constant increases.

The gradual increase in the dielectric constant with increasing total conductor concentration may be attributed to the decrease of the air space distance between the conducting clay minerals (or organic matter) that behave as a capacitor, especially for low total conductor concentration. The capacitance gradually increases as the total conductor concentration increases [44–46].

Fig. 10 shows the complex impedance plane variation of samples with different concentrations. Generally, for low concentrations of the conductor an arc in the impedance plane can be seen and this arc is contracted to a part of semicircle with the increase of conductor concentrations. This arc may be contracted to a semicircle at the higher conductor concentrations [47]. Samples 1 and 5 may be compared to each other; they show an arc and a depressed semicircle (or may be a semicircle), respectively. The increase in real impedance may be attributed to an increase of continuous conductor paths between electrodes.

Generally, the conductivity increases with the increase of total conductor concentration, which may be attributed to an increase of relatively conducting paths between the electrodes. The conductivity increases sharply, at low conductor concentrations, and at higher conductor concentrations it begins to saturate as the conductivity reaches its maximum value. At high frequencies (1 MHz) the conductivity shows a value of the order of 10^{-2} S/m (Fig. 8).

Generally, the dielectric constant increases with the increase of total conductor concentration, which may be attributed to a decrease of distances between the relatively more conducting grains. This occurred directly due to the increase of relatively more conducting concentrations [48]. The distances between relatively more conducting grains decrease until it vanishes and the first conductor continuous path begins to be formed, then with the increase of relative conducting concentrations the dielectric constant begins to decrease again (this is not seen in our group of samples). This is what is called the critical

Table 2 The geoaccumulation indexes of the studied samples.

Range	Degree of pollution	Elements in the studied samples
<0	Unpolluted	
0–1	Unpolluted to moderately polluted	Si, Ti, Al, Fe, Mn, Mg, Sr, Na, K and Pb
1–2	Moderately polluted	Cu, Ni, Rb and Cr
2–3	Moderately to strongly polluted	P
3–4	Strongly polluted	Zn and Ca
4–5	Strongly to very strongly polluted	
>5	Very strongly polluted	V, Zr, Cd and Mo

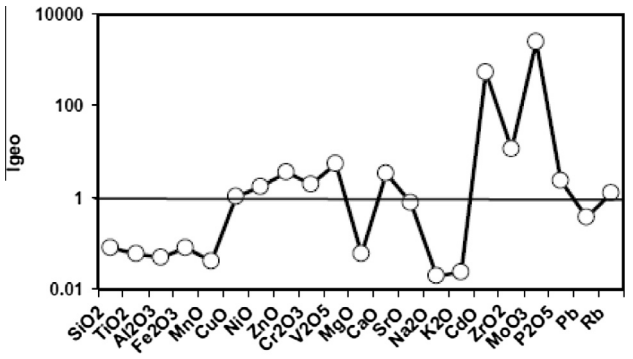

Figure 7 Shows the geoaccumulation index for the studied shale samples.

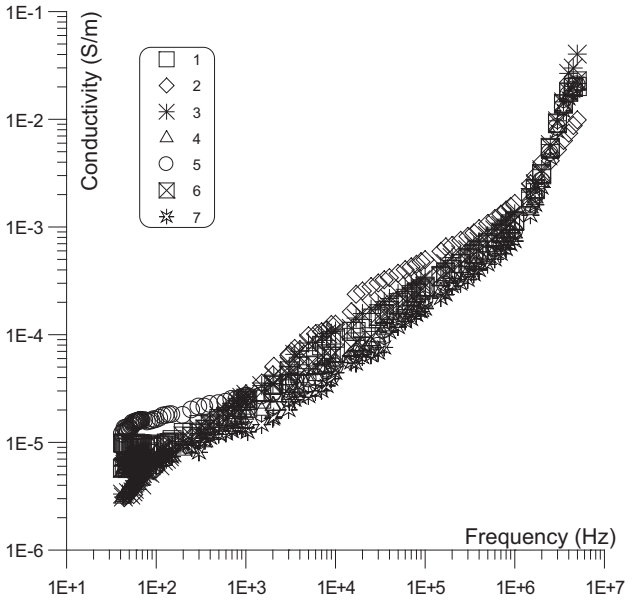

Figure 8 Shows the variation of the conductivity with frequency.

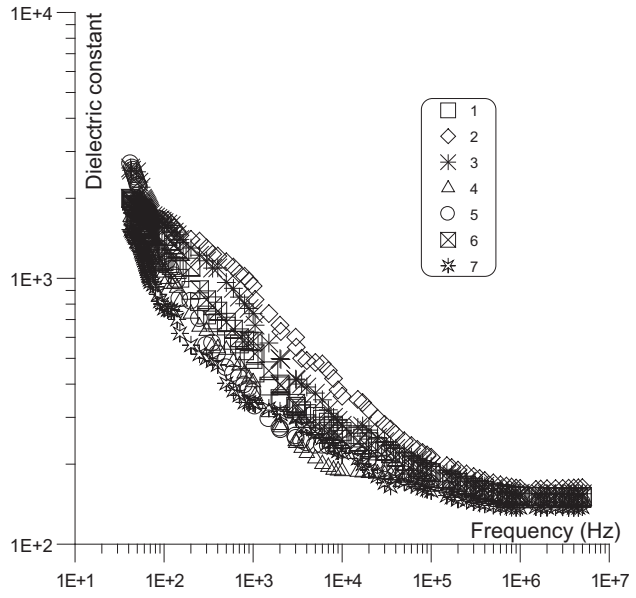

Figure 9 Shows the variation of the dielectric constant with frequency.

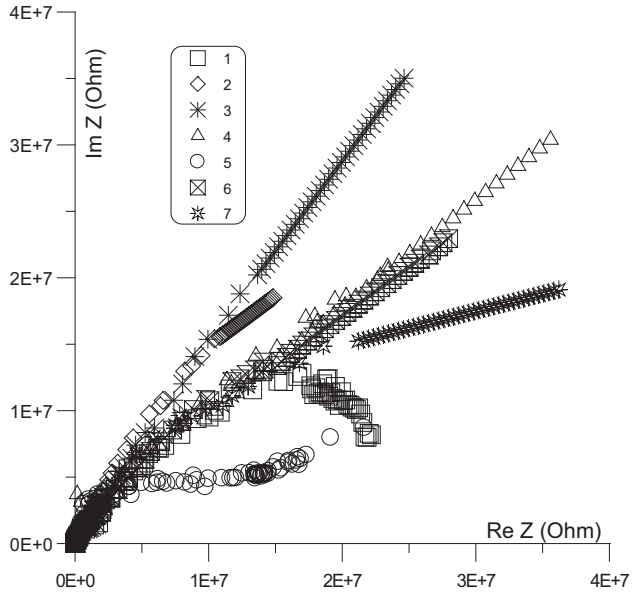

Figure 10 Shows the variation of the real and imaginary impedance.

concentration. Dielectric constant increases for relatively higher conductor concentrations to reach a value of 200 (samples 1, 4, 9 and 7).

With the changes in texture (grain size, grain shape, concentration and porosity) from one sample to another, curves changed, even if they have the same concentration, because the texture is not the same [49].

5. Conclusion

Electrical, petrographical and geochemical discussions and interpretations were made in order to explore the relation between geochemical composition of measured samples (carbonates that contain clays minerals, quartz grains and organic mater) and texture. Electrical properties were done using non-polarizing electrode at room temperature (~18 °C) and at a relative atmospheric humidity of (~35%) in the frequency range from 42 Hz to 5 MHz.

The Duwi Formation in the Quseir–Safaga area consists of phosphorite, shale, siliceous claystone, glauconitic sandstone, chert, dolostone, marl and reefal limestone. Mineralogicaly, the bulk of marine black shales are composed mainly of calcite, apatite, quartz and pyrite. The dominated clay minerals in the studied clay fraction are mainly well crystalline Na- montmorillonite, mixed layer of montmorillonite- illite and minor illite. They are texturally classified as phosphatic marly mudstone. They are represented as detrital, authigenic and highly mature. The black shale is rich in organic matter and sulfide. The studied shales contain high concentrations of some trace elements such as V, Zn, Zr, Cr, Mo, Ni and Cd, which added significant value to the studied shales. The mineralogical and geochemical compositions revealed that the studied marine black shales were derived from more mafic. There may be an additional source from felsic source rocks provenance in a prevailing intensive chemical weathering conditions. They are deposited under relatively euxinic to anoxic reducing marine conditions coupled with hydrothermal solutions. The parent rocks of the studied shales are mainly of basaltic provenance affected by chemical weathering. The calculated environmental parameters reveal that the of Quseir–Safaga area is varying between unpolluted to very strong polluted, which may be attributed to the intensive weathering of the source rocks. Consequently, the studied black shales are probably derived from the basement terrains in the Red Sea Hills (west of Quseir area), and transported through Wadi Quleh. The basement rocks are composed of metagabbro diorite, serpentinite and metavolcanic as a source of mafic minerals. On the other hand, the observed enrichment of Zr could be attributed to the granite and the Nubian Sandstones.

The electrical responses of individual components of samples (texture) change when combinations of components are changed and may be due to interactions on their surfaces. Also, these values are influenced by the concentrations of conductive and/or insulating particles in the samples especially at low frequencies. Dielectric constant and conductivity increases with the increase of relative conductor concentration (may be iron or clay). Dielectric constant decreases with frequency increase while conductivity increases with frequency increase. The dielectric properties may be attributed to an increase of the conductor concentration. As conductive clustering materials are increased and the thickness of insulating gaps between conductive clusters decreases, an increase in the dielectric constant of samples is shown. Conductors and insulators combine together to give the net final degree of conduction or insulation in the samples.

References

[1] R. Said, The Geology of Egypt, A.A. Balkema, Rotterdam, Netherlands, 1990, 734 p.
[2] M.M. Gomaa, Ann. Geophys. 51 (5/6) (2008) 801–811.
[3] M.M. Gomaa, M. Elsayed, Geophys. Prospect. 57 (1) (2009) 141–149.
[4] M.M. Gomaa, Induced Polarization Study on Iron Ore Bearing Rock Samples (Ph. D. thesis), Cairo University, Egypt, 2004.

[5] M.M. Gomaa, E.A. Abou El-Anwar, J. Geophys. Eng. 12 (2015) 292–302, http://dx.doi.org/10.1088/1742-2132/12/3/292.
[6] R.J. Knight, A.L. Endres, Geophysics 55 (1990) 586–594.
[7] M.M. Gomaa, A. Shaltout, M. Boshta, Mater. Chem. Phys. 114 (1) (2009) 313–318.
[8] H.M. Baioumy, S.I. Ismael, Int. J. Coal Geol. 83 (2010) 35–45.
[9] M.M. Gomaa, Geophys. Prospect. 57 (2009) 1091–1100.
[10] M.M. Gomaa, P. Alikaj, Marine Geophys. Res. 30 (4) (2010) 265–276, http://dx.doi.org/10.1007/s11001-010-9092-y.
[11] M.M. Gomaa, in: B. Veress, J. Szigethy (Eds.), Horizons in Earth Science Research, vol. 6, Nova Science Publishers, Inc., 2011, pp. 83–146, ISBN 978-1-61470-462-1.
[12] V. Ciobota, W. Salama, J. Paul-Vargas, T. Nicolae, R. Petra, A. El Kammar, S. Rania, M. Morsy, J. Popp, Spectrochim. Acta Part A: Mol. Biomol. Spectrosc. 118 (2014) 42–47.
[13] K.K. Turekian, in: K.H. Wedepohl (Ed.), Handbook of Geochemistry, II/3, Springer, Berlin, 1978 (28-K-1–28-L-3).
[14] E.A. Abou El-Anwar, M.S. El-Sayed, Bull. NRC, Egypt 32 (5) (2008) 511–536.
[15] E.A. Abou El-Anwar, Int. Conf. Geol. Eng. 80 (2011) 1315–1325 (Paris, France, 24–26 August).
[16] E.A. Abou El-Anwar, Geol. Soc. Egypt 56 (2012) 33–48.
[17] S.R. Taylor, S.M. McLennan, The Continental Crust: Its Composition and Evolution, Blackwell, Oxford, 1985, 312 p.
[18] M. El-Shafeiy, B. Daniel, A. El-Kammar, A. El-Barkooky, M. Wagreich, M. Omar, J. Peckmann, Cretaceous Res. 50 (2014) 38–51.
[19] K.E. Peters, C.C. Walters, J.M. Moldowan, The Biomarker Guide, Biomarkers and Isotopes in Petroleum Systems and Human History, second ed., I, Cambridge University Press, United Kingdom, 2005, 476 p.
[20] T. Cao, Z. Song, S. Wang, X. Cao, Y. Li, X. Jia, Mar. Pet. Geol. 61 (2015) 140–150.
[21] M. Blumenberga, V. Thiela, W. Riegela, K. Linda, R. Joachim, Precambrian Res. 196–197 (2012) 113–127.
[22] R.A. Berner, R. Raiswell, Geology 12 (1984) 365–368.
[23] D. Gross, R.F. Sachsenhofer, A. Bechtel, L. Pytlak, B. Rupprecht, E. Wegerer, Mar. Pet. Geol. 59 (2015) 1–21.
[24] B. Liu, Y. Wang, X. Su, H. Zheng, Chemie der Erde (2013).
[25] S.S. El-Wekeil, E.A. Abou El Anwar, J. Appl. Sci. Res. 9 (8) (2013) 4781–4798.
[26] M. Steiner, E. Wallis, B.D. Erdtmann, Y.L. Zhao, R.D. Yang, Palaeogeogr. Palaeoclimatol. Palaeoecol. 169 (2001) 165–191.
[27] T. Angerera, R. Kerrichb, G. Steffen, Precambrian Res. 224 (2013) 110–128.
[28] R. Cox, D.R. Lower, R.L. Cullers, Geochim. Cosmochim. Acta 59 (1995) 2919–2940.
[29] D.J. Wronkiewicz, K.C. Condie, Geochim. Cosmoch. Acta 51 (1987) 2401–2416.
[30] H.W. Nesbitt, G.M. Young, Nature 299 (1982) 715–717.
[31] S.M. McLennan, S. Hemming, D.K. McDaniel, G.N. Hanson, in: M.J. Johnson, A. Basu (Eds.), Processes Controlling the Composition of Clastic Sediments, Geological Society of American Special Paper, USA, 1993, pp. 21–40.
[32] J.H. Wei, S.Y. Wang, G.F. Lu, Geochemistry 21 (1995) 99–102.
[33] C.M. Fleurance, F. Malartre, J. Reyx, Palaeogeogr. Palaeoclimatol. Palaeoecol. 369 (2013) 201–219.
[34] M.D. Lewan, Geochim. Cosmochim. Acta. 48 (1984) 2231–2238.
[35] P. Schulte, L. Schwark, P. Stassen, T.J. Kouwenhoven, A. Bornemann, P.S. Robert, Palaeogeogr. Palaeoclimatol. Palaeoecol. 371 (2013) 9–25;
J.A. Valdivieso-Ojeda, M.A. Huerta-Diaz, F. Delgadillo-Hinojosa, Chem. Geol. 363 (2014) 341–354.
[36] B. Peng, A. Rate, Z. Song, C. Yu, X. Tang, S. Xie, X. Tu, T. Changyin, Appl. Geochem. 51 (2014) 191–203.
[37] J.Z. Xu, B. Peng, C.X. Yu, G. Yang, X.Y. Tang, C.Y. Tan, S.R. XieTan, X.L. TU, Z.C. Bao, M.J. Quan, M. Xiao, Environ. Earth Sci. 70 (1) (2013) 175–190.
[38] G. Müller, Geology. J. 2 (1969) 108–118.
[39] K. Loska, D. Wiechula, L. Korus, Environ. Int. 30 (2004) 159–165.
[40] A.A. Shaltout, M.M. Gomaa, M. Wahbe, X-ray Spectrom. 41 (2012) 355–362.
[41] A.L. Efros, B.I. Shklovskii, Phys. Status Sol. No.76 (1976) 475–489.
[42] T.M. Levitskaya, B.K. Sternberg, Radio Sci. 35 (2) (2000) 371–383.
[43] R. Knight, J. Geomagn. Geoelec. 35 (1983) 767–776.
[44] A. Jonscher, J. Phys. D: Appl. Phys. 32 (1999) R57–R70.
[45] T. Chelidze, Y. Gueguen, Geophys. J. Int. 137 (1999) 1–15.
[46] T. Chelidze, Y. Gueguen, C. Ruffet, Geophys. J. Int. 137 (1999) 16–34.
[47] F.A. Grant, J. Appl. Phys. 29 (1958) 76–80.
[48] R.J. Knight, A. Nur, Geophysics 52 (1987) 644–654.
[49] E.A. Abou El-Anwar, M.M. Gomaa, Geophys. Prospect. (2012), http://dx.doi.org/10.1111/j.1365-2478.2012.01087.x.